PROBABILITY OF DETECTION OF FLAWS IN A GAS TURBINE ENGINE COMPONENT USING ELECTRIC CURRENT PERTURBATION

Gary L. Burkhardt and R.E. Beissner

Southwest Research Institute
6220 Culebra Road
San Antonio, Texas 78284

INTRODUCTION

In an exploratory development program, the Electric Current Perturbation (ECP) method was optimized for inspection of typical F-100 gas turbine engine components (disks and seals).[1,2] A primary objective was to achieve high reliability for the detection of flaws (fatigue cracks) at the retirement-for-cause (RFC) target flaw size of 0.010 in. long x 0.005 in. deep. Probability of detection (POD) data for surface flaws in blade slots of an F-100 first stage fan disk were estimated from experimentally determined probability density functions (PDF's) for background and flaw signals. The POD as a function of flaw size was estimated from these data.

EXPERIMENTAL SETUP

Experimental data for calculation of POD were obtained from blade slots in an F-100 first stage fan disk. Factors considered in the selection of blade slots included the availability of a statistically significant number of blade slots from which background signals could be obtained, as well as "worst-case" inspection conditions due to background noise from the Ti 6-2-4-6 material and peened surfaces. A computer-controlled, laboratory breadboard scanning system was used to obtain the ECP data. Figure 1 shows the F-100 first stage fan disk (Ti 6-2-4-6) positioned in the scanning system. The ECP probe was mounted on an air bearing which allowed the probe to be scanned without physical contact with the specimen surface and at a controlled liftoff. The blade slot configuration and scan direction are shown, schematically, in Figure 2. The flaws were located at the tangency point of the 0.350 in. radius, approximately 0.50 in. from the edge of the blade slot. Since equivalent ECP signals are obtained from fatigue cracks and EDM slots of the same size[3], half-penny shaped EDM slots were used to simulate fatigue cracks. Dimensions of the two EDM slots were 0.0182 in. long x 0.0105 in. deep and 0.0105 in. long x 0.0058 in. deep.

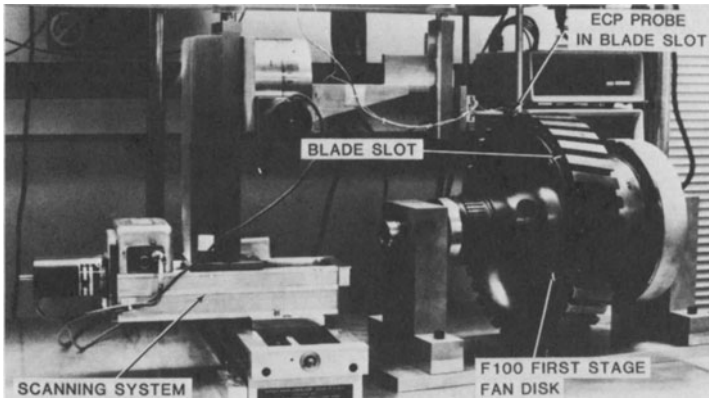

Fig. 1. ECP laboratory breadboard scanning system with F-100 first stage fan disk in place.

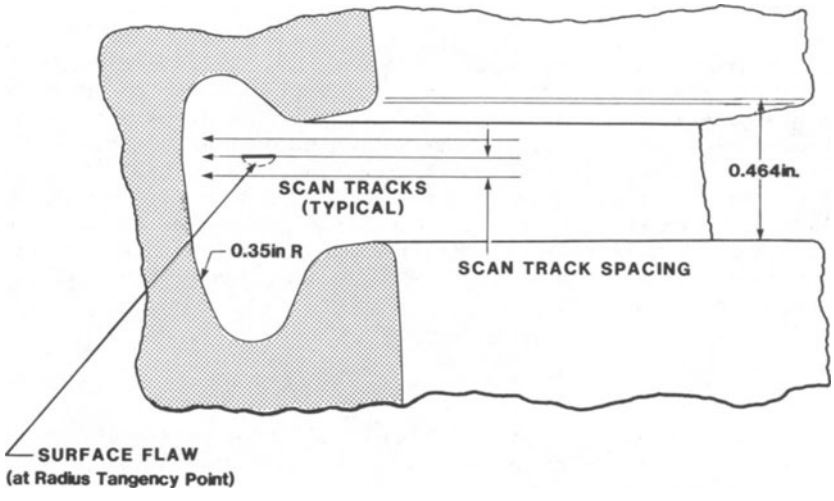

Fig. 2. Scan configuration for blade slots.

STATISTICAL ANALYSIS OF FLAW DETECTION

Despite all efforts to insure repeatability, experimental measurements of flaw signal amplitudes are never exactly the same, in the strict mathematical sense, over a set of repeated scans of the same flaw. Instead, the signal amplitudes thus obtained form a distribution of values ranging from a minimum to a maximum and having some mean, or average, value. If one were to calculate the number of times a given amplitude was observed divided by the total number of scans, and then plot the resulting data as a function of signal amplitude, the curve obtained would be the probability density function for signal amplitudes from that particular flaw size. A similar probability density function for noise or background signals can be defined in much the same way. Two such probability density functions, one for the flaw signal and the other for noise, are shown schematically in Figure 3.

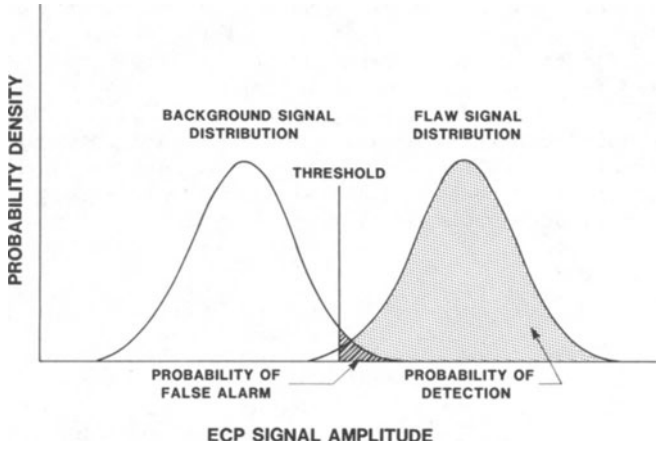

Fig. 3. Schematic illustration of probability density functions for signals and background noise.

In an inspection situation one would hope that the probability density function (PDF) for flaw signals would lie well to the right (in the sense of Figure 3) of the PDF for noise, so that a given signal amplitude could be unambiguously interpreted as either a flaw signal or noise. In such an ideal case all flaws would be detected and there would be no false alarms from background signals that appear to indicate the presence of a flaw.

In practice this ideal situation is realized only for very large flaws in the presence of very weak noise signals. Usually the PDF's for flaw signals and noise overlap to some extent, as indicated in Figure 3. It is the extent of overlap, or, more precisely, the areas under the PDF curves in the overlap region, that determine the reliability of the inspection method. This is because what one usually does in a situation where signal and noise PDF's overlap to a significant extent is decide, first of all, how often one can tolerate false indications of the presence of a flaw. This decision determines a threshold value for signal amplitude, below which signals will be interpreted as noise and above which signals will be interpreted as flaw indications. The area under the noise PDF to the right of the threshold value is then the probability that background noise will give a false indication of the presence of a flaw. At the same time the choice of a threshold value also determines the probability of flaw detection, because the area under the flaw signal PDF to the right of the threshold is the probability of detection. It also determines the probability that flaws will be missed, which is equal to the area under the signal PDF to the left of the threshold. Thus the extent of overlap of the flaw signal and noise PDF's, and the choice of a threshold amplitude for flaw detection, play a critical role in determining the reliability of an NDE method.

SIGNAL AND NOISE DATA FOR BLADE SLOTS

For the purpose of this analysis, signal and noise amplitudes are defined as peak-to-peak voltages as indicated in Figure 4. Flaw signal data was obtained by recording the amplitudes measured in 30 repeated

scans directly over the 0.0105 in. X 0.0058 in. flaw. The resulting PDF is shown as a histogram on the right side of Figure 5. The smooth curve is a Gaussian fit to the PDF determined from the mean and standard deviation of the data. Noise data were obtained from single scans in unflawed regions in each of 30 blade slots in the disk. The amplitude recorded for each scan was the maximum noise signal observed in a 1.0 in. scan length. The PDF resulting from these data is shown on the left side of Figure 5. Due to the relatively rough, peened blade slot surface, the background signals are larger than might be expected from other engine parts*, and the noise PDF is therefore shifted closer to the flaw signal PDF.

Fig. 4. Definition of flaw and background signal amplitudes.

The distributions shown in Figure 5 represent the best possible flaw detection situation because signal data were obtained from scans directly over the flaw where the amplitude is greatest. In a practical situation, of course, one does not even know if flaws exist, much less their exact locations. What is done, therefore, is to scan the piece in a raster-like fashion, as in Figure 2, with the distance between scan tracks determined from statistical data to give an acceptable probability of detection and false alarm rate. Under such conditions the scan track-to-flaw distance can be assumed to be equally likely to be any distance from zero (directly over the flaw) to one-half the spacing between scan tracks.

*Although the sources of the background signals are not fully understood, a limited investigation indicates that a higher background is obtained from parts with peened surfaces than from those with smoother surfaces.[2]

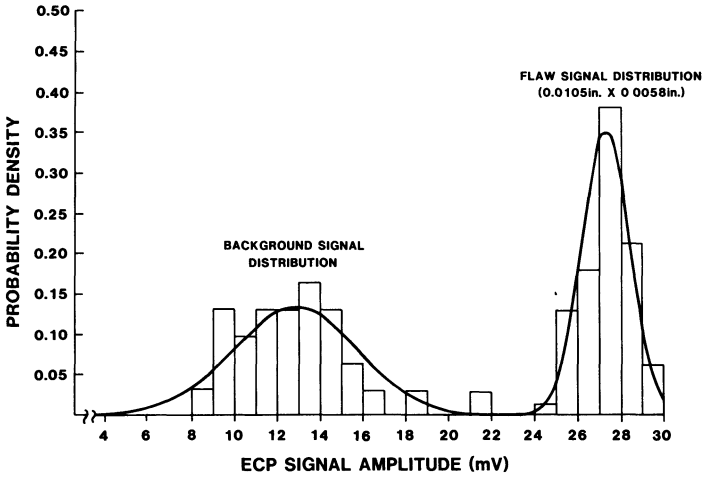

Fig. 5. Signal and background probability density functions for blade slots.

To obtain data representative of a practical inspection procedure, additional flaw signal data were obtained for scan tracks displaced in 0.001 in. increments from 0.0 in. to 0.007 in., each repeated 10 times. Data from the displaced scans (0.001 in. to 0.007 in.) were given twice the weight of data from scans directly over the flaw to account for the fact that in an actual inspection the flaw is equally likely to be on either side of the scan track. The full set of data thus approximates the distribution of signal amplitudes obtained from an inspection in which scan tracks are 0.014 in. apart, because the flaw location, which is equally likely to be anywhere in the scan pattern, can then be no more than 0.007 in. from a scan track. The full set of data therefore determines a PDF corresponding to an inspection procedure in which scan tracks are spaced 0.014 in. apart. This PDF is shown as a histogram in Figure 6, along with the corresponding Gaussian fit.

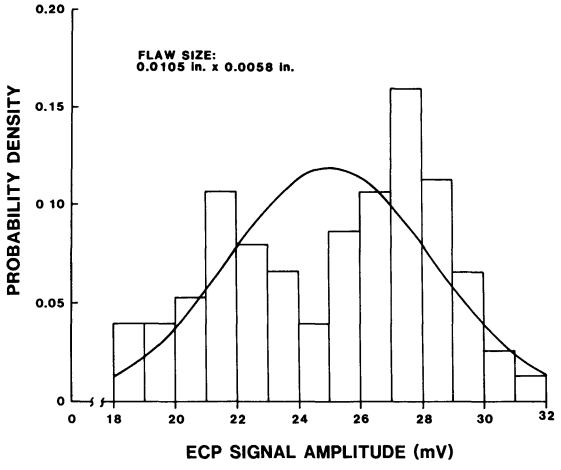

Fig. 6. Flaw signal probability density function for a 0.0105 in. x 0.0058 in. flaw with 0.014 in. scan track spacing.

Mean signal amplitudes are plotted as a function of distance from the flaw in Figure 7. From this plot it can be seen that the signal amplitude decreases only 10% over distances from 0.0 to 0.004 in. from the flaw. Thus, if scan tracks were taken to be 0.008 in. apart, one would expect the corresponding PDF to closely approximate the ideal PDF obtained from scans directly over the flaw. For this reason a second PDF, based on the 5 scan tracks (each repeated 10 times) from 0.0 to 0.004 in. from the flaw, was also generated. The result is shown in Figure 8.

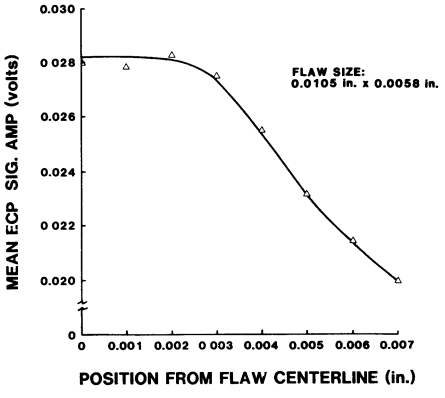

Fig. 7. Mean signal amplitude for a 0.0105 in. x 0.0058 in. flaw as a function of flaw-to-scan track spacing.

CALCULATIONS OF PROBABILITY OF DETECTION

The PDF's shown in Figures 6 and 8 correspond to two different inspection procedures but only one flaw size. To extend the analysis to other flaw sizes, the following approximations were introduced: (1) The standard deviation is independent of flaw size. This means that the shape of the PDF is assumed to be the same regardless of the size of the flaw. (2) The mean signal amplitude is proportional to flaw area. This approximation shifts the PDF to the left or right by an amount proportional to the area of the face of the flaw; it is based on a linear amplitude-area scaling relationship which has been confirmed previously.[2,4]

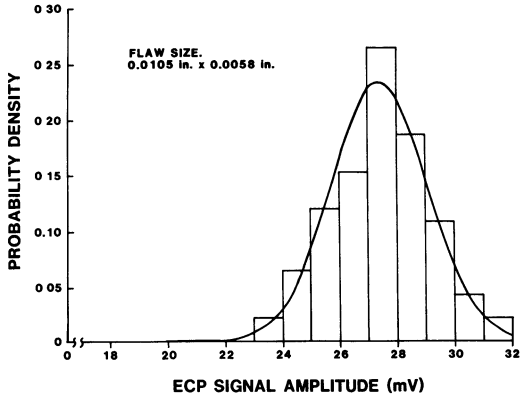

Fig. 8. Flaw signal probability density function for a 0.0105 in. x 0.0058 in. flaw with 0.008 in. scan track spacing.

For the calculation of probabilities of detection, false alarm probabilities of 10^{-6}, 10^{-5}, 10^{-4} and 10^{-3} were chosen as representative of the values one might choose for a blade slot inspection. These numbers were then used to determine the four corresponding threshold amplitudes from the noise PDF shown in Figure 5. Probabilities of detection were then calculated as previously described for flaw lengths ranging from 0.008 in. to 0.012 in. for flaw signal PDF's corresponding to both the 0.008 and 0.014 in. scan track spacings. Because all detection probabilities were very close to 1.0 for 0.012 in. flaws, there was no need to extend the analysis to larger flaws.

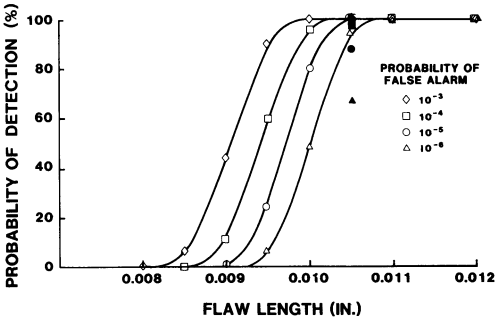

Fig. 9. Probability of detection detail for 0.008 in. scan track spacing. Open symbols are based on the approximation discussed in the text; solid symbols are based on actual experimental data.

To simplify the computations, Gaussian fits to the PDF's were used instead of actual PDF data for most of the estimates of probability of detection. As a check on the validity of this approximation, additional calculations were performed for the 0.0105 x 0.0058 in. flaw using the actual, experimentally determined PDF data. The results for both 0.014 and 0.008 in. scan track spacings are shown in Figures 9 and 10, which are plots of all calculated probabilities of detection based on the Gaussian approximation, as a function of flaw size. Data obtained directly from the PDF histograms are also shown in these figures.

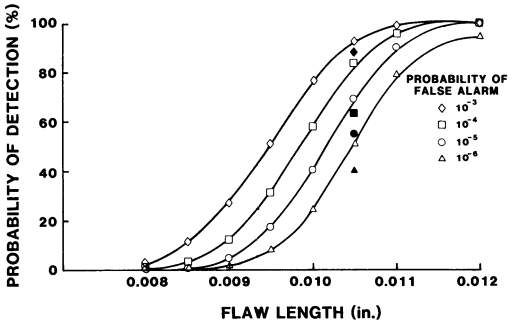

Fig. 10. Probability of detection detail for 0.014 in. scan track spacing. Open symbols are based on the approximation discussed in the text; solid symbols are based on actual experimental data.

The very sharp rise in the probability of detection data plotted in Figures 9 and 10 means that virtually all flaws with areas slightly greater than that of 0.010 x 0.005 in. target flaw size will be detected with either the 0.014 to the 0.008 in. scan spacing. For flaw lengths in the 0.008 to 0.012 in. range, Figures 9 and 10 show the sensitivity of the probability of detection to the choice of false alarm probability and, comparing the two figures, to the choice of scan track spacing. These figures also show that the use of the Gaussian approximation to PDF's, which was largely a matter of convenience, tends to give detection probabilities that are somewhat greater than one would obtain from experimentally determined PDF data. Although differences are significant, it was decided that the data set was too limited to warrant further study. Thus, these data should be regarded as preliminary estimates, with the differences between probabilities of detection as calculated from actual PDF data and Gaussian fits to the data giving some indication of the uncertainty in the estimates. Clearly, much more data are needed for a more accurate assessment of probability of detection.

In spite of such uncertainties, the high POD values obtained from the study are very encouraging (see Figures 9 and 10). It is particularly gratifying to note that the experiments were performed under what was considered to be a "worst case" condition in which background noise from the rather rough blade slot surface is greater than might be expected with other engine components. It is clear that much better detectability can be achieved in components with background noise lower than that of these blade slots.

CONCLUSIONS

1. Depending on the scan track spacing, the POD is approximately 100% for flaw lengths of about 0.011 in. to 0.013 in.

2. A higher POD for smaller flaws would be obtained in parts with background noise lower than obtained in the F-100 first stage fan disk blade slots.

ACKNOWLEDGMENTS

The authors wish to thank Mr. Floyd Balter for fabrication of ECP probes and Mr. Thomas Doss for assistance with data acquisition. Support of this work was provided by the Air Force Wright Aeronautical Laboratories, Materials Laboratory.

REFERENCES

1. Gary L. Burkhardt, Felix N. Kusenberger, and R.E. Beissner, "Electric Current Perturbation Inspection of Selected Retirement-for-Cause Turbine Engine Components," Review of Progress in Quantitative Nondestructive Evaluation, 3B, Donald O. Thompson and Dale E. Chimenti, Eds., Plenum Publishing Corp., pp. 1377-1387, 1984.

2. R.E. Beissner, Gary L. Burkhardt, and Felix N. Kusenberger, "Exploratory Development on Advanced Surface Flaw Detection Methods, Final Report, Contract No. F33615-82-C-5020, Air Force Systems Command, June 1984.

3. C.M. Teller and Gary L. Burkhardt, "Application of the Electric Current Perturbation Method to the Detection of Fatigue Cracks in a Complex Geometry Titanium Part," Review of Progress in Quantitative Nondestructive Evaluation, 2B, Donald O. Thompson and Dale E. Chimenti, Eds., Plenum Publishing Corp., pp. 1203-1217, 1983.

4. R.E. Beissner, M.J. Sablik, and C.M. Teller, "Electric Current Perturbation Calculations for Half-Penny Cracks," Review of Progress in Quantative Nondestructive Evaluation, 2B, Donald O. Thompson and Dale E. Chimenti, Eds., Plenum Publishing Corp., pp. 1237-1254.